Journal of Saudi Chemical Society (2016) **20**, 343–348

King Saud University

Journal of Saudi Chemical Society

www.ksu.edu.sa
www.sciencedirect.com

ORIGINAL ARTICLE

Synthesis of CNTs/CuO and its catalytic performance on the thermal decomposition of ammonium perchlorate

Ping Cui *, **An-juan Wang**

School of Chemistry and Chemical Engineering of Anhui University of Technology, Anhui Key Laboratory of Coal Clean Conversion & Utilization, Ma'anshan 243002, Anhui, China

Received 4 July 2014; revised 25 September 2014; accepted 25 September 2014
Available online 5 October 2014

KEYWORDS

CNTs/CuO;
Ammonium perchlorate;
Catalysis

Abstract Copper oxide (CuO) nanoparticles were successfully deposited on carbon nanotubes' (CNTs) surface via complex-precipitation method, the nanocomposite was characterized by transmission electron microscopy (TEM), scanning electron microscopy (SEM), X-ray photoelectron spectroscopy (XPS), X-ray powder diffraction (XRD), Raman spectroscopy, Fourier transform infrared (FT-IR) and Brunauer–Emmett–Teller (BET). The catalytic performance of CNTs/CuO on ammonium perchlorate (AP) decomposition was analyzed by differential thermal analyzer (DTA), the DTA results showed its excellent catalytic effect on AP decomposition, as 8 wt.% CNTs/CuO was added in AP, the second exothermic peak temperature decreased by 158 °C. Such composite may be a promising candidate for catalyzing the AP thermal decomposition.

1. Introduction

Ammonium perchlorate (AP), a white crystalline substance, is the most commonly used oxidizer in composite solid propellants (CSPs). Obviously, the thermal decomposition characteristic of AP affects the performance of CSPs. Generally speaking, the lower the decomposition temperature of AP, the shorter the delay time of propellant ignition, the higher the combustion rate and the better the performance of CSPs [1]. Over the past several decades, numerous catalysts have been employed to decrease the decomposition temperature of AP [2–5]. The results suggested that the decomposition process of AP was remarkably sensitive to the catalysts and the nanometer sized catalysts possessed better catalytic property as compared with their bulk size. Among the metal oxide catalysts, copper oxide (CuO) nanoparticles (NPs) showed particular catalytic effect due to their high concentration of dislocations and large surface areas [6]. However, nanoparticles are easy to aggregate due to their large surface energy, which will further affect their catalytic performance.

Extensive attention has been paid on CNTs since their first discovery [7] in many fields, such as catalyst [8], lithium ion batteries [9] and solar cells [10]. For its application in catalyst field, it should be noted that the perfect structure along its tube

* Corresponding author.
E-mail addresses: 1178878420@qq.com, mhgcp@126.com (P. Cui).
Peer review under responsibility of King Saud University.

ELSEVIER Production and hosting by Elsevier

http://dx.doi.org/10.1016/j.jscs.2014.09.010

wall allows them to be the excellent dispersing-supporters for the NPs [11–13]. Our earlier work [14] showed that the CNTs/Cu exhibited better catalytic effect on AP thermal decomposition than the simple mixture of CuNPs and CNTs did, indicating CNTs can improve the catalytic performance of CuNPs as a supporter. However, CNTs/CuO has not been reported to catalyze the thermal decomposition of AP. Herein, in our work CNTs/CuO nanocomposite was prepared, compared with the simple mixture of CuONPs and CNTs, CNTs/CuO nanocomposite exhibited higher catalytic activity for AP thermal decomposition.

2. Experimental

2.1. Preparation of CNTs

Catalytic chemical vapor deposition (CCVD) method was employed to synthesize CNTs. In a typical experiment, the volume of benzene (carbon source) and thiophene (growth stimulant) was 150 and 1 ml, respectively. Catalyst (ferrocene, about 2 g) was uniformly spread on an alumina boat placed in a horizontal tube furnace. After the temperature of the furnace was raised to 1170 °C under a flow of nitrogen gas at a rate of 200 ml/min, hydrogen gas was introduced at a rate of 380 ml/min for 15 min. The as-prepared CNTs were functionalized by 100 ml concentrated mixed acids (H_2SO_4/HNO_3 = 3:1) under stirring condition at 75 °C for 2 h.

2.2. Synthesis of CNTs/CuO composite

Firstly, CNTs, SDS and copper chloride($CuCl_2$) were dispersed in 50 ml distilled water under ultrasound condition for 30 min, subsequently, superfluous aqueous ammonia(e) was added in the solution, then sodium hydroxide (NaOH) was added into the solution stirred at 50 °C drop by drop, after that, the solution was stirred at 50 °C for another 1 h. Finally, the sample was filtered, washed with distilled water several times, dried and calcinated in muffle furnace at 400 °C for 2 h. CuONPs were prepared following the same procedure above without adding CNTs at the beginning.

2.3. Characterization

X-ray powder diffraction (XRD) analysis of the samples was carried out with a German D8ADVANCE X-ray diffractometer with Cu Kα radiation (k = 1.54056 Å). X-ray photoelectron spectroscopy (XPS) was performed with an American Thermo ESCALAB 250 electron spectrometer using Al K irradiation. Morphology of the samples was investigated using a transmission electron microscopy (TEM) on a FEI instrument (T-12 TENcai) subjected to an acceleration voltage of 120 kV and a scanning electron microscopy (SEM) using a JEOL 35. Raman spectra of the samples were recorded in the frequency range of 200–2000 cm^{-1} using a Raman spectrometer (JY HR-800 type) with a laser excitation line at 532 nm. Fourier transform infrared (FT-IR) spectra were recorded on a NicdeT 740 spectrometer using pressed KBr pellets to test the chemical bonding of the samples from 500 to 3750 cm^{-1}. The Brunauer–Emmett–Teller (BET) surface area of as-synthesized samples was determined by using an instrument of the Beckman Coulter Co. Ltd., USA.

2.4. Catalytic analysis

Thermal decomposition study of pure AP and AP with catalysts was performed with the differential thermal analyzer (DTA, TA instrument SDT-Q600) under a heating rate of 20 °C/min in a static N_2 atmosphere with α-Al_2O_3 as reference material. Sample of approximately 1.5 mg was taken. The mass content of CNTs/CuO composite added in AP was 4 wt.%, the catalytic performance of the mixture of CNTs and CuONPs was also carried out in the same way as comparison. At the same time, CNTs/CuO with mass content of 1 wt.% and 8 wt.% was selected to study the effect of the mass content of CNTs/CuO on AP thermal decomposition.

3. Results and discussion

Fig. 1a shows the SEM image of CNTs/CuO, in which CuONPs are well dispersed along the CNTs surface. Fig. 1b shows the TEM image of CNTs/CuO, which further proves the uniform disperse of CuONPs on CNTs, also indicates the uniform thickness of the loading layer. It should also be mentioned that although the TEM specimen suffers from long time sonication, perfect loading of CuONPs on CNTs can still be seen clearly, indicating the strong force between CuONPs and CNTs [15].

Fig. 2 illustrates the XRD patterns of CNTs (Fig. 2a) and the synthesized CNTs/CuO composite (Fig. 2b). For the XRD pattern of CNTs, three characteristic peaks at 26.41°, 43.6° and 53.12° correspond to the (002), (101) and (004) inter-planar spacing of CNTs, respectively. For the XRD pattern of CNTs/CuO, the intensity of the three characteristic peaks of CNTs are weakening or disappearing, maybe caused by the fine loading of CuONPs on CNTs surface. Besides the diffraction peaks of CNTs, other strong diffraction peaks could be assigned to CuO (JCPDS Card No. 80-1916). From the Scherrer formula, it can be calculated that the average size of CuO on CNTs is 25 nm approximately. To further confirm the Cu species and its content on CNTs surface, XPS analysis was carried out (Fig. 3). Fig. 3a shows the XPS result of CNTs/CuO, from which C, O and Cu can be easily detected, according to the surface element analysis, the content of C, O and Cu is 45.07%, 34.57% and 20.36%, respectively. Fig. 3b shows the XPS result of Cu 2p, the two main peaks at about 933.6 and 953.6 eV are associated with the binding energy of Cu $2p_{3/2}$ and Cu $2p_{1/2}$, respectively, which confirm the formation of Cu^{2+}. Fig. 3c shows O 1s XPS curves, where the non-lattice oxygen species (e.g., hydroxyl group, adsorbed oxygen species) with peak position at 531.2 eV (marked as I) is evident. The peak at 529.6 eV (marked as II) corresponds to the surface lattice oxygen [16]. The content of non-lattice oxygen and lattice oxygen is 39.01% and 60.99% in the detection layer of the XPS analyses, respectively, which indicate that 20.36% Cu exists in the form of CuO.

To have a far better knowledge of the surface structure of the composite, Raman spectra of CNTs (Fig. 4a) and CNTs/CuO (Fig. 4b) are presented. As shown in Fig. 4b, the peak at 292 cm^{-1} is attributed to the Ag mode and the peaks at 342 and 627 cm^{-1} are attributed to the Bg mode of CuO. Both the spectra display the peak at about 1350 cm^{-1} (D-band) associated with the vibrations of carbon atoms in the disordered graphite structure and the peak at about 1585 cm^{-1}

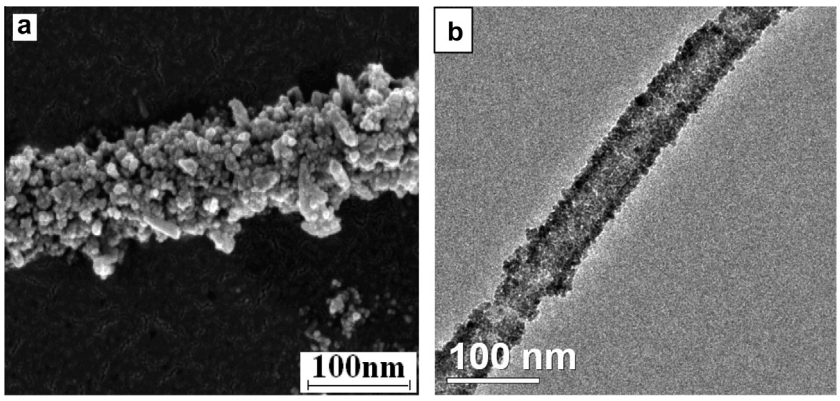

Figure 1 SEM (a) and TEM (b) images of CNTs/CuO.

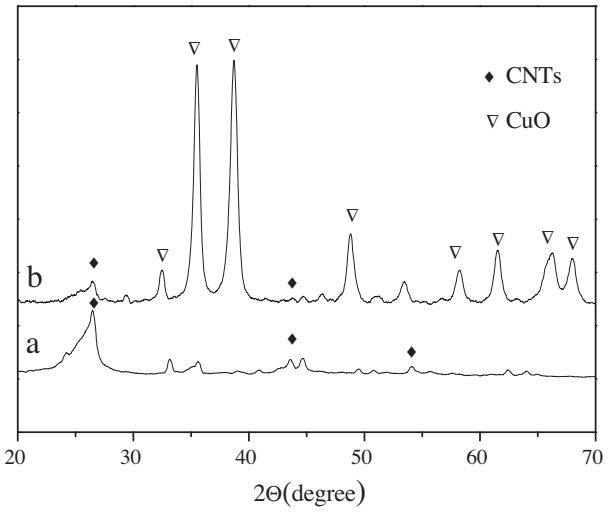

Figure 2 XRD patterns of pure CNTs (a) and CNTs/CuO (b).

(G-band) which corresponds to the E2g mode of graphite. It is known that the ratio of the intensity of D-band to G-band (I_D/I_G) suggests the defect density in CNT samples. As shown in Fig. 4, the value of I_D/I_G is 1.03 for CNTs and then decreases to 1.02 after CuO loading. This means that CuO NPs prefer anchoring onto the defect structures rather than to the perfect sites of CNTs, which is consistent with the study of other researchers [17–19]. In addition, the defects on CNTs surface may have a profound impact upon electronic transport properties and produce electron acceptor-like states within graphitic materials [19–21].

The preparation process of CNTs/CuO can be inferred as follows. Firstly, carboxylic and hydroxyl groups were introduced onto CNTs during the functionalization process, as proved by the bands at 1719 and 3439 cm^{-1} shown in Fig. 5a. When superfluous $NH_3{\cdot}H_2O$ was added, complex $[Cu(NH_3)_4]^{2+}$ was formed, afterward, $[Cu(NH_3)_4]^{2+}$ was attached to CNTs through the reaction between amide and carboxylic groups [22], as it can be proved, no band corresponding to the carboxylic groups can be detected in the FTIR spectra of CNTs/CuO nanocomposite (Fig. 5b). As NaOH solution was added slowly, $Cu(OH)_2$ precipitate was formed in situ and stabilized by the chemisorption and Van der Waals interactions between $Cu(OH)_2$ and CNTs [23]. Under heating and stirring conditions, $Cu(OH)_2$ was converted to CuO. During the preparation process of pure CuONPs, it can be observed that the color of the solution changed from blue-green to blue, then to black finally, which can also prove the formation process of CNTs/CuO described above to some extent.

BET analyses were performed to investigate the specific surface area of the samples. For pure CuONPs and CNTs, the specific surface area is 17.6 and 48.7 $m^2\,g^{-1}$ respectively, while the specific surface area of CNTs/CuO is 80.0 $m^2\,g^{-1}$, much higher than that of pure CuONPs and CNTs. Specific surface area is one of the important methods to characterize the catalytic properties of materials. Generally, the higher the specific surface area of the catalyst is, the better its catalytic performance is. The high specific surface area of CNTs/CuO indicates CNTs could effectively prevent the aggregation of CuONPs, which may lead to their excellent catalytic performance.

Fig. 6 shows the thermal decomposition process of pure AP and AP with catalysts. As shown in Fig. 6a, the thermal decomposition of pure AP has apparently three stages [2–6,24]. In the first stage, the endothermic peak temperature appears at about 245 °C, ascribed to its crystal transition from orthorhombic to cubic. In the second stage, the exothermic peak temperature appears at about 328.1 °C which is attributed to the partial decomposition of AP and the formation of an intermediate product. While the third peak, also the main exothermic peak, appears at relatively higher temperature 478 °C, indicating the further and complete decomposition of the intermediate products. As the catalysts were added (Fig. 6a,b), the thermal decomposition of AP in the second and the third stage became significantly different while little change can be observed in the first stage, which is similar with the effect of other catalysts on the AP thermal decomposition [2–5]. As the mixture of CuO and CNTs was added (Fig. 6a), the two exothermic peaks merge into one peak, the second exothermic peak temperature decreases by 135 °C, as CNTs/CuO (Fig. 6a) was added, the two exothermic peaks also merge into one peak, and the second exothermic peak temperature decreases by 145 °C, indicating that CNTs can further improve the catalytic performance of CuO particles for AP thermal decomposition as a supporter. In addition, as shown in Fig. 6b, relatively high content of CNTs/CuO (1 wt.%,

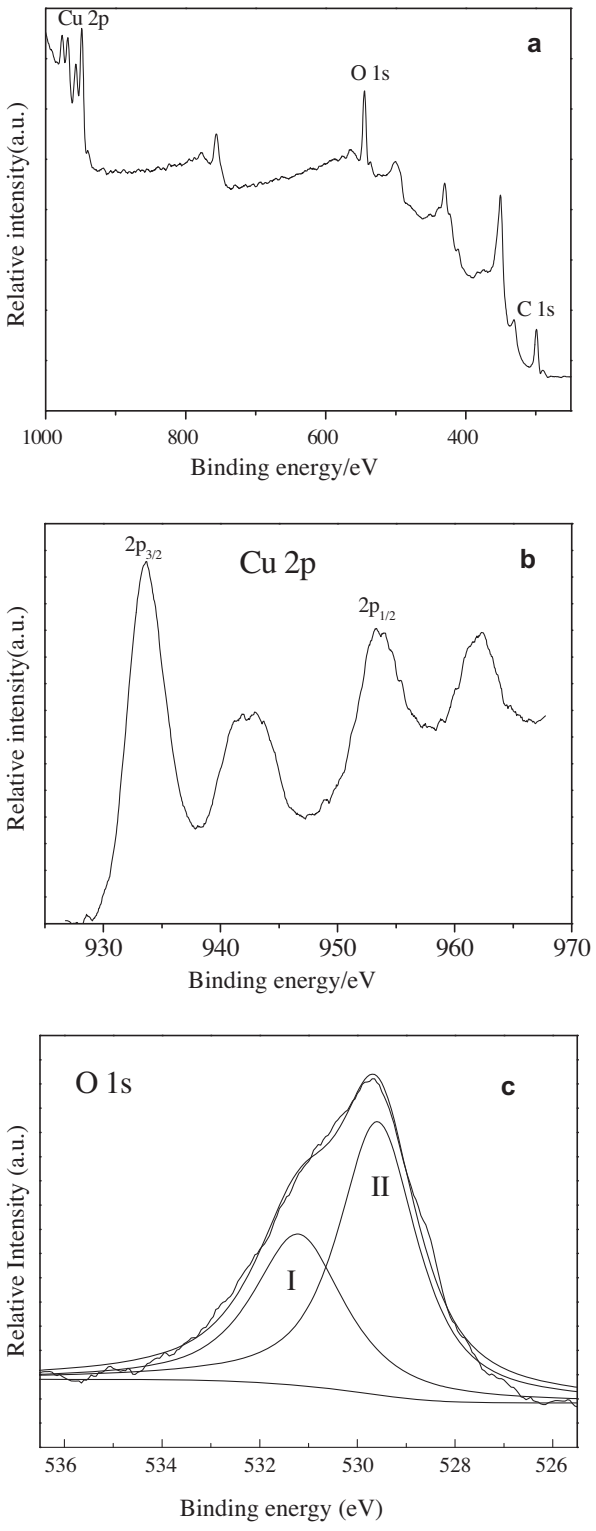

Figure 3 XPS pattern of CNTs/CuO (a), Cu 2p (b) and O 1s (c).

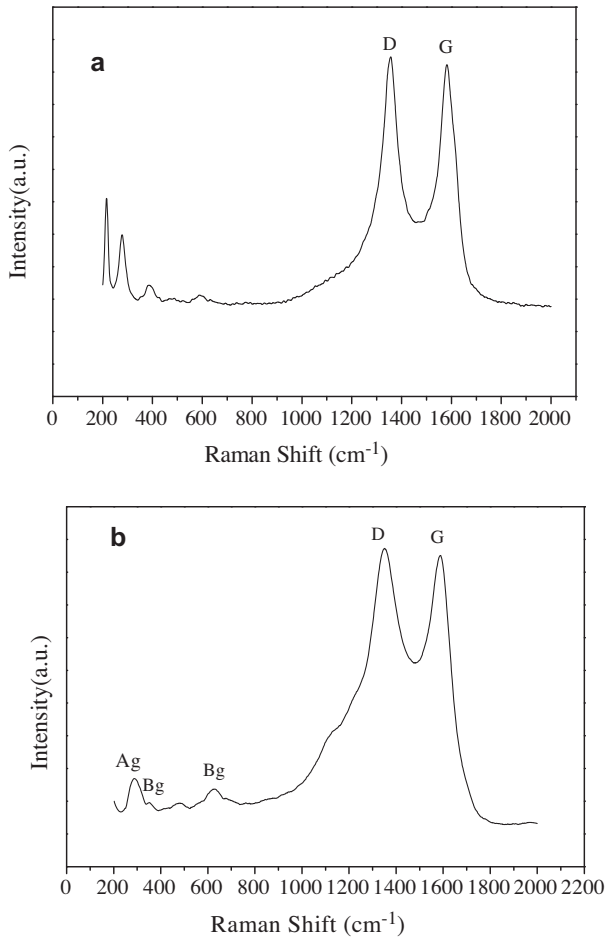

Figure 4 Raman spectra of CNTs (a) and CNTs/CuO (b).

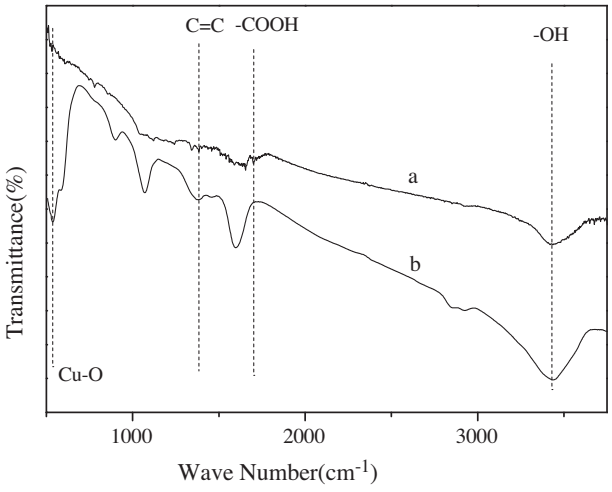

Figure 5 FTIR spectra of pure CNTs (a) and CNTs/CuO (b).

4 wt.% and 8 wt.%) favors the further decrease of the second exothermic peak temperature of AP. As 8 wt.% CNTs/CuO was added, the second exothermic peak temperature decreases by 158 °C, indicating that such catalyst may be a promising candidate to prepare the excellent-performance of solid rocket propellants.

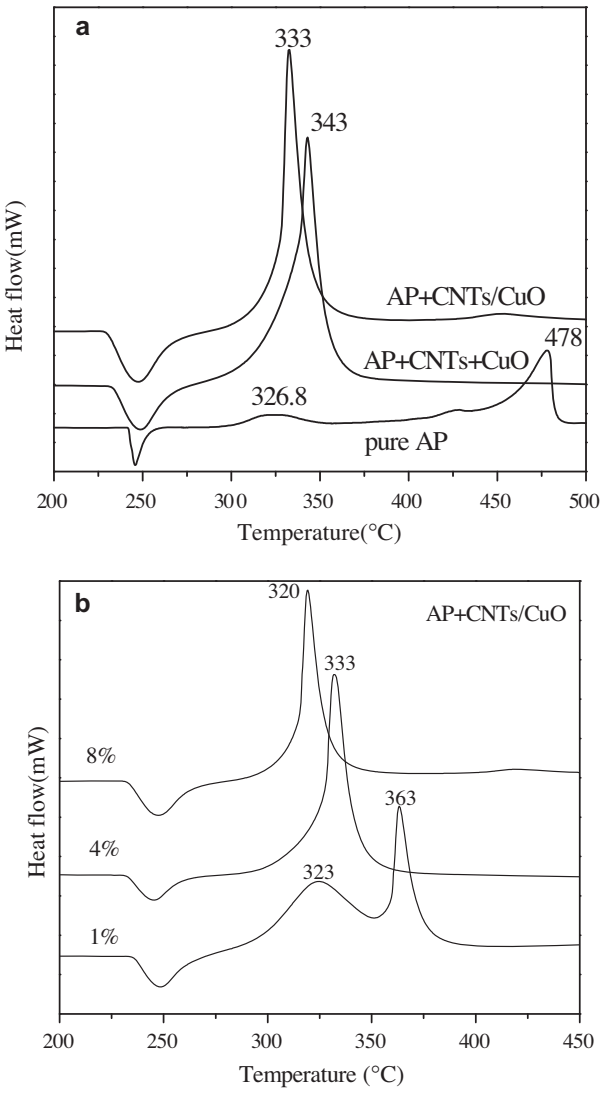

Figure 6 DTA curves of the thermal decomposition of pure AP and AP with catalysts (a and b).

4. Conclusions

This work has prepared CNTs/CuO nanocomposites and studied its catalytic effect on the thermal decomposition of ammonium perchlorate. The results showed that with the addition of CNTs/CuO nanocomposite in AP, the decomposition temperature of AP decreased significantly. As 8 wt.% nanocomposite was added in AP, only the second exothermic peak can be seen, and its corresponding temperature decreased by 158 °C.

References

[1] Z.X. Yu, L.F. Chen, L.D. Lu, X.J. Yang, X. Wang, DSC/TG-MS study on in situ catalytic thermal decomposition of ammonium perchlorate over CoC_2O_4, Chin. J. Catal. 30 (2009) 19–23.

[2] D.V. Survase, M. Gupta, S.N. Asthana, The effect of Nd_2O_3 on thermal and ballistic properties of ammonium perchlorate (AP) based composite propellants, Prog. Cryst Growth Charact. Mater. 45 (2002) 161–165.

[3] R. Dubey, P. Srivastava, I.P.S. Kapoor, G. Singh, Synthesis, characterization and catalytic behavior of Cu nanoparticles on the thermal decomposition of AP, HMX, NTO and composite solid propellants, Part 83, Thermochim. Acta 549 (2012) 102–109.

[4] F.J. Xiao, X.A. Sun, X.F. Wu, J.C. Zhao, Y.J. Luo, Synthesis and characterization of ferrocenyl-functionalized polyester dendrimers and catalytic performance for thermal decomposition of ammonium perchlorate, J. Organomet. Chem. 713 (2012) 96–103.

[5] Prajakta R. Patil, V.N. Krishnamurthy, Satyawati S. Joshi, Effect of nano-copper oxide and copper chromite on the thermal decomposition of ammonium perchlorate, Propellants Explos. Pyrotech. 33 (2008) 266–270.

[6] Anuj A. Vargeese, K Muralidharan, Kinetics and mechanism of hydrothermally prepared copper oxide nanorod catalyzed decomposition of ammonium nitrate, Appl. Catal. A: Gen. 447–448 (2012) 171–177.

[7] S. Iijima, Helical microtubules of graphitic carbon, Nature 354 (1991) 56–58.

[8] Y.P. Zhang, Y.C. Jiao, Y.S. Yang, C.L. Li, Ligand-free catalytic system for the synthesis of diarylethers over Cu_2O/Cu-CNTs as heterogeneous reusable catalyst, Tetrahedron Lett. 54 (2013) 6494–6497.

[9] Q.X. Guo, P.F. Guo, J.T. Li, H. Yin, J. Liu, F.L. Xiao, et al, Fe_3O_4–CNTs nanocomposites: inorganic dispersant assisted hydrothermal synthesis and application in lithium ion batteries, J. Solid State Chem. 213 (2014) 104–109.

[10] J. Yan, M.J. Uddin, T.J. Dickens, O.I. Okoli, Carbon nanotubes (CNTs) enrich the solar cells, Sol. Energy 96 (2013) 239–252.

[11] S.F. Zheng, J.S. Hu, L.S. Zhong, L.J. Wan, W.G. Song, In situ one-step method for preparing carbon nanotubes and Pt composite catalysts and their performance for methanol oxidation, J. Phys. Chem. C 111 (2007) 11174–11179.

[12] G.W. Yang, G.Y. Gao, C. Wang, C.L. Xu, H.L. Li, Controllable deposition of Ag nanoparticles on carbon nanotubes as a catalyst for hydrazine oxidation, Carbon 46 (2008) 747–752.

[13] X.J. Zhang, W. Jiang, D. Song, J.X. Liu, F.S. Li, Preparation and catalytic activity of Ni/CNTs nanocomposites using microwave irradiation heating method, Mater. Lett. 62 (2008) 2343–2346.

[14] P. Cui, F.S. Li, J. Zhou, W. Jiang, Preparation of Cu/CNT composite particles and catalytic performance on thermal decomposition of ammonium perchlorate, Propellants Explos. Pyrotech. 31 (2006) 452–455.

[15] N. Li, Z.F. Geng, M.H. Cao, L. Ren, X.Y. Zhao, B. Liu, et al, Well-dispersed ultrafine Mn_3O_4 nanoparticles on graphene as a promising catalyst for the thermal decomposition of ammonium perchlorate, Carbon 54 (2013) 124–132.

[16] J.F. Xu, W. Ji, Z.X. Shen, S.H. Tang, X.R. Ye, D.Z. Jia, et al, Preparation and characterization of CuO nanocrystals, J. Solid State Chem. 147 (1999) 516–519.

[17] J.A. Rodriguez-Manzo, O. Cretu, F. Banhart, Trapping of metal atoms in vacancies of carbon nanotubes and graphene, ACS Nano 4 (2010) 3422–3428.

[18] S.J. Kim, Y.J. Park, E.J. Ra, K.K. Kim, K.H. An, Y.H. Lee, et al, Defect-induced loading of Pt nanoparticles on carbon nanotubes, Appl. Phys. Lett. 90 (2007) 023114.

[19] S.Q. Song, S.J. Jiang, Selective catalytic oxidation of ammonia to nitrogen over CuO/CNTs: the promoting effect of the defects of CNTs on the catalytic activity and selectivity, Appl. Catal. B: Environ. 117–118 (2012) 346–350.

[20] T. Savage, S. Bhattacharya, B. Sadanadan, J. Gaillard, T.M. Tritt, Y.P. Sun, et al, Photoinduced oxidation of carbon nanotubes, J. Phys. Condens. Matter 15 (2003) 5915.

[21] A.K. Chakraborty, R.A.J. Woolley, Y.V. Butenko, V.R. Dhanak, L. Siller, M.R.C. Hunt, A photoelectron

spectroscopy study of ion-irradiation induced defects in single-wall carbon nanotubes, Carbon 45 (2007) 2744–2750.
[22] X.Y. Wang, B.Y. Xia, X.F. Zhu, J.S. Chen, S.L. Qiu, J.X. Li, Controlled modification of multiwalled carbon nanotubes with ZnO nanostructures, J. Solid State Chem. 181 (2008) 822–827.
[23] S.M. Abbas, S.T. Hussain, S. Ali, F. Abbas, N. Ahmad, N. Ali, et al, One-pot synthesis of a composite of monodispersed CuO nanospheres on carbon nanotubes as anode material for lithium-ion batteries, J. Alloys Compd. 574 (2013) 221–226.
[24] J.N. Wang, X.D. Li, R.J. Yang, Preparation of ferric oxide/carbon nanotubes composite nano-particles and catalysis on burning rate of ammonium perchlorate, Chin. J. Explos. Propellants 29 (2006) 44–47.